https://doi.org/10.17221/534/2025-PSE

Sensing weeds and crops using thermal and hyperspectral imaginary

Hana Vašková[1]*, *Alois Bilavčík*[2], *Milan Kroulík*[3], *Jan Lukáš*[1]

[1]*Functional Diversity in Agro-Ecosystems, Czech Agrifood Research Centre, Prague 6 – Ruzyně, Czech Republic*
[2]*Plant Physiology and Cryobiology Team, Czech Agrifood Research Centre, Prague 6 – Ruzyně, Czech Republic*
[3]*Department of Agricultural Machines, Faculty of Engineering, Czech University of Life Sciences, Suchdol, Prague, Czech Republic*
**Corresponding author: hana.vaskova@carc.cz*

Citation: Vašková H., Bilavčík A., Kroulík M., Lukáš J. (2026): Sensing weeds and crops using thermal and hyperspectral imaginary. Plant Soil Environ., 72: 146–154.

Abstract: The availability of new sensor technologies, such as thermal and hyperspectral imaging, enables early-stage weed detection and species identification and density estimation, both of which are crucial for effective weed management. Thermal imaging successfully distinguished between dicotyledonous (oilseed rape, pea, *Stellaria media*, *Triplerospermum inodorum*, *Veronica persica*) and monocotyledonous species (barley, wheat, sorghum and *Echinochloa crus-galli*) except *Amaranthus retroflexus*, during early growth stages. The most pronounced differences in hyperspectral reflectance occurred at 550 nm, where five distinct plant groups were recognisable (sum of squares = 0.7604, *F*-value = 105.1). The highest hyperspectral reflectance was recorded for oilseed rape, followed by *Stellaria media*. The same trend was found for the normalised difference index (NDI), which also showed five distinct groups. These findings indicate that thermography and hyperspectral imaging have strong potential as effective tools for supporting weed detection in precision agriculture; however, further research and field validation are required before routine implementation in agricultural practice.

Keywords: sensor; thermography; hyperspectral technology; plant detection

Sensor technologies have become key drivers of innovation in modern agriculture, enabling detailed descriptions of factorial, spatial, and temporal heterogeneity. Combined with GIS tools, they allow sophisticated monitoring of biotic and abiotic stressors, supporting data-based decisions that can be translated into application maps. The quality and effectiveness of implemented measures can then be evaluated using these technologies. Although thermal and hyperspectral imaging are not new, recent developments in sensor design have made high-resolution cameras more accessible, driven by growing industrial interest and declining costs. These imaging systems are now widely used in crop production for various purposes, including phenotyping, pathogen and pest detection, soil texture mapping, estimation of residue cover, monitoring and mapping of crop yield (Khanal et al. 2017, Espinoza et al. 2017, Maimaitijiang et al. 2017). Such analyses are based on differences in canopy architecture, leaf morphology, and physiology. Furthermore, thermal and hyperspectral cameras can detect changes in photosynthetic activity (Shirzadifar 2018), often linked to stomatal regulation.

Supported by the Project NAZV, Project No. QK22010348 "Autonomous systems as tools for integrated vegetable production." and by the Institutional Project MZE RO0825.

https://doi.org/10.17221/534/2025-PSE

Current weed management practices largely rely on RGB sensor technology, as demonstrated in several studies (e.g., Raja et al. 2020). This approach offers many advantages, including cost-effectiveness, high resolution, user-friendly application, wide availability or real-time operation (Su 2020, Murad et al. 2023). However, RGB systems are limited by their restricted spectral range, light sensitivity, and susceptibility to environmental conditions. They primarily rely on visual features such as leaf shape, size, and colour, making species-level identification of taxonomically and morphologically similar species nearly impossible (Wang et al. 2019). This limitation highlights the need for alternative or complementary methods that can provide species-level discrimination.

Hyperspectral analyses on plant species have so far been conducted primarily in forest ecosystems, where identifying species composition and density requires substantial effort. For example, an analysis of variance conducted by Pu et al. (2008) showed that 30 selected spectral variables effectively differentiated 11 tree species, with the strongest separation at 550 nm, attributed to differences in chlorophyll concentration (Gitelson and Merzlyak 1998). Similarly, Pantazi et al. (2016) demonstrated that plant species could be distinguished by using hyperspectral imaging. More recent studies have extended this approach to invasive plant detection (Dmitriev et al. 2022).

However, the use of only a single wavelength is not appropriate due to optical errors, external and environmental conditions, and the overall setup of hyperspectral sensing (Nansen et al. 2025). In this study, the normalised difference index (NDI, Chen et al. 2021) was used, calculated from reflectance values at two visible wavelengths (550 nm and 490 nm), corresponding to the green and blue spectral regions, which enable discrimination between healthy and diseased plants and also allow differentiation among individual plant species.

Thermal analyses have been successfully applied in urban forestry, arboriculture and fruit production (Stajnko et al. 2006), as well as in crop production. Thermal cameras can detect mechanical damage to plants, stress, fungal infection (Catena and Catena 2008), insect infestation (Shoba et al. 2024), and even herbicide resistance in weeds (Eide et al. 2021). Both hyperspectral and thermal imaging offer major advantages, as they enable non-invasive, real-time evaluation of plant health and physiology.

To date, no study has empirically demonstrated that weeds and crops differ in their reflected temperature. Thus, it is necessary to determine whether significant differences in temperature exist among plant species. For hyperspectral analysis, this study included both weed and crop species that had not been tested in similar experiments.

The need for accurate weed detection, recognition, and precision control is increasingly important as herbicide costs rise and environmental concerns intensify. These include off-target spray drift (Taylor et al. 2004), water contamination (Primel et al. 2005, Mesnage and Zaller 2021), and biodiversity loss (Barros-Rodriguez et al. 2021, Esposito et al. 2023). Modern sensing technology, such as thermal and hyperspectral imaging, could play a key role in addressing these challenges. The primary aim of this study is to evaluate differences in apparent leaf temperature and hyperspectral reflectance between targeted weed and crop species to determine their efficacy for early, precise weed identification.

MATERIAL AND METHODS

Plant material. In this study, five weed species (*Veronica persica* Poiret, *Tripleurospermum inodorum* (L.) Sch. Bip., *Echinochloa crus-galli* (L.) P. B., *Stellaria media* (L.) Vill, *Amaranthus retroflexus* L.) and five crops (spring barley – cv. Sebastián, winter wheat – cv. Butterfly, pea – cv. ESO, oilseed rape – cv. Angelico, sorghum – cv. Ruzrok) were analysed. These weed plants were selected for their high agricultural relevance (Grime, Hodgson, and Hunt 1990). For each species, 12 plants were grown individually in pots (7.5 × 7.5 cm at the top, 8 cm high), as a growing medium, a horticultural substrate type A (Rašelina Soběslav, Soběslav, Czech Republic), which is made from a mixture of peat, finely ground limestone and the multi-component mineral fertiliser Cererit. Each pot contained one plant. Plants were cultivated and imaged under control conditions (12 h light/12 h dark photoperiod, constant temperature of 20 °C). Illumination was provided by an LED lamp (Lumatek ATS, 300W PRO (ATTIS), 2.7 µmol/J). Plants were watered according to each species' requirements, supplying water only from the bottom of the pots to avoid surface wetting.

Seeds of crop species were obtained commercially (Seed Service s.r.o., 2022). Weed seeds were collected manually at full maturity.

Because weed control is most effective during the early phenological stages (Page et al. 2012, Marschner et al. 2024), all plants were photographed at the two-true-leaf stage.

https://doi.org/10.17221/534/2025-PSE

Thermal imaging: data acquisition and analysis. Thermal images were acquired by Workswell WIC640 camera (Workswell, Prague, Czech Republic) equipped with an uncooled VOx microbolometer (640 × 512 pixels), operating in the long-wave infrared spectral range of 7.5–13.5 μm, with a thermal sensitivity of approximately 30 mK and radiometric temperature measurement capability. The thermal images were taken in the same climatic chamber where the plants were growing, to minimise temperature changes caused by manipulation. Thermal images were taken from 30 cm from the fixed position, in a vertical view, to achieve the most practical use, i.e., attachment to the tractor. Thermal imaging was conducted within a single measurement session to minimise inter-session variability. Before data acquisition, the thermal camera was allowed to stabilise for an appropriate warm-up period. Non-uniformity correction (NUC) was performed according to the manufacturer's recommendations. All images were acquired using identical camera settings. Thermal images were analysed with ThermoLab Desktop (Workswell, Prague, Czech Republic). Each thermal image captured only one pot containing one plant to maximise the number of pixels available for analysis. For Poaceae species, thermal reflectance was analysed as a line of four pixels along the first true leaf to account for leaf morphology. For all other species, four randomly selected pixels forming a square on the second leaf were analysed. These pixels were selected manually in the middle of the leaf (in the lamina), avoiding major veins. The apparent leaf temperature of the single leaf was counted as an arithmetic mean. No special soil cover was used during thermal imaging.

To minimise the variability in apparent leaf temperature (camera-reported values) and to standardise environmental conditions, pots were placed on sand and watered with tap water at a uniform temperature throughout sampling. Two analytical approaches were tested: uncorrected apparent leaf temperature and apparent leaf temperature corrected by a temperature index. The correction index was calculated as the ratio of apparent leaf temperature to wet sand-reflected temperature (T plant/T sand). Sand temperature was measured along a line of four pixels.

Temperature differences among species were evaluated by analysis of variance (ANOVA), with temperature as the dependent variable and species identity as the independent variable. Post hoc comparisons were performed using Tukey's multiple comparisons of means at a 95% family-wise confidence level. The null hypothesis stated that apparent leaf temperature and correction index did not differ significantly among species. All analyses were conducted in R software (Team 2022) using the stats and multcomp packages, with a significance level of $\alpha = 0.05$.

Hyperspectral imaging: data acquisition and analysis. The images were obtained with a Specim IQ camera (Specim Spectral Imaging Ltd., Oulu, Finland) from 30 cm. In thermal imaging, each image contained only one pot with one plant to maximise the number of pixels for analysis. The hyperspectral camera operated in the VNIR range (400–1 000 nm, CMOS sensor) with 204 spectral bands and a spectral resolution (FWHM) of 7 nm. Based on manufacturer specifications, the resulting radiometric performance provides a high signal-to-noise ratio across the VNIR range, making it suitable for vegetation. A dark reference was acquired automatically by the Specim IQ camera before data acquisition to correct for sensor dark current. A white reference measurement was performed using a calibrated diffuse reflectance standard before image acquisition. The integration time was set automatically by the camera to optimise signal levels and avoid saturation. Illumination was provided by two halogen lamps (OSRAM, Display/Optic lamp 3200 K, 1000V). Images were processed in Specim IQ Studio software (Specim Spectral Imaging Ltd., Oulu, Finland), and spectral reflectance data were extracted using Scyven software (Scyllarus Visualisation Environment; Habili and Oorloff 2015). Raw radiance data were converted to reflectance using Scyven software by normalising each pixel spectrum to the white reference after dark current correction. For each pot, five randomly selected central pixels of the second leaf were analysed for spectral reflectance. To reduce background interference by soil reflection and moss growth, the top of the pot was covered with black paper coated on one side with plastic film (facing the soil surface). A circular hole was cut in the centre to allow the plant to grow through without any stress.

To identify wavelengths showing the greatest interspecific variation, the analysis of variance (ANOVA) was performed for each wavelength. The wavelength exhibiting the maximum *F*-statistic (≈550 nm; this region was selected a posteriori because it showed the greatest separation in band-wise screening, consistent with the literature) was subsequently selected for detailed analysis using the vegetation index NDI. NDI was used because of the imaging system's technical limitations to eliminate effects

https://doi.org/10.17221/534/2025-PSE

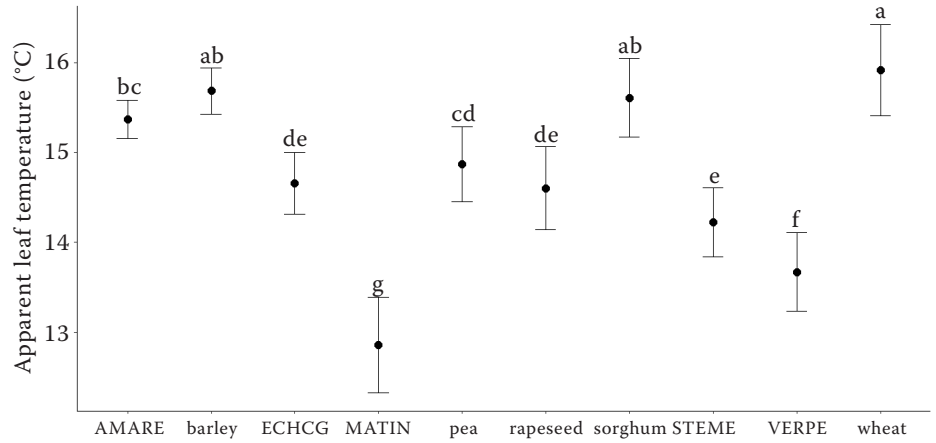

Figure 1. Mean of apparent leaf temperature (reported by camera). Each point represents the mean apparent leaf temperature, and the vertical bars represent standard deviation (SD). Different letters above the means indicate statistically significant differences ($P < 0.05$). AMARE – *Amaranthus retroflexus*; ECHCG – *Echinochloa crus-galli*; MATIN – *Tripleurospermum inodorum*; STEME – *Stellaria media*; VERPE – *Veronica persica*

such as a short distance between the samples and the camera or the angle of illumination of the plant leaves. The normalised difference index (NDI) was calculated as NDI = $(R_{550} - R_{490})/(R_{550} + R_{490})$, also known as HBCI9 – hyperspectral biochemical index 9 (Thenkabail et al. 2024).

ANOVA (for wavelength 550 and for NDI index) was conducted with hyperspectral reflectance 550 nm (obtained from Scyven software) or values of NDI as the dependent variable and species as the independent variable. The ANOVA results were then analysed using Tukey's multiple comparisons of means (95% family-wise confidence level). The null hypothesis stated that there was no significant difference in spectral reflectance or NDI values among species. All analyses were performed in R using the stats, multcomp, tidyr, and ggplot2 packages, with a significance level of $\alpha = 0.05$.

RESULTS

Thermal emission. The apparent leaf temperature of the species varied significantly, $F_{(9, 127)} = 14.70$, $P < 0.001$, with a sum of squares of 115.115 for species and 21.659 for residuals. The residual standard error was 0.413 (Figure 1). The highest mean of apparent

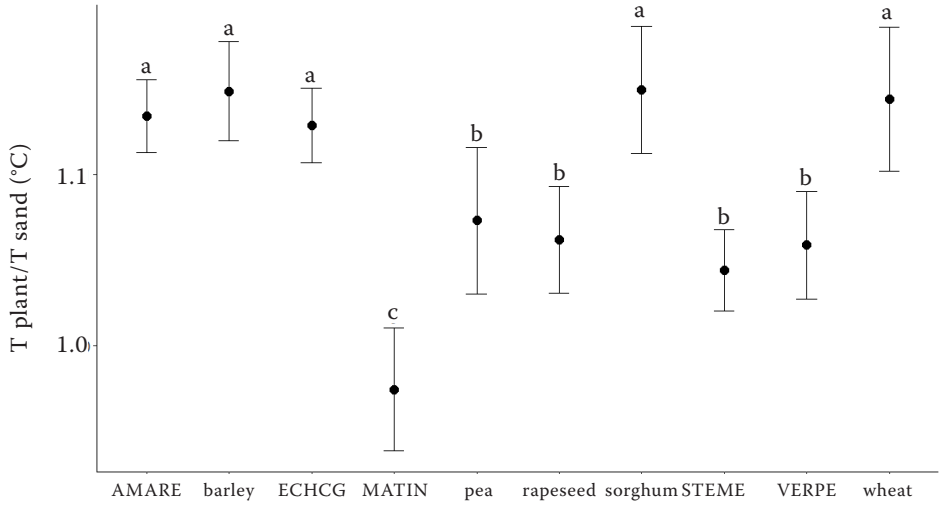

Figure 2. Mean of correction index (T plant/T sand) for different species. Each point represents the mean index, and the vertical bars represent standard deviation (SD). Different letters above the means indicate statistically significant differences ($P < 0.05$). AMARE – *Amaranthus retroflexus*; ECHCG – *Echinochloa crus-galli*; MATIN – *Tripleurospermum inodorum*; STEME – *Stellaria media*; VERPE – *Veronica persica*

https://doi.org/10.17221/534/2025-PSE

leaf temperature was recorded for wheat (mean = 15.916 °C, SD = 0.507 °C), followed by barley (mean = 15.684 °C, SD = 0.259 °C). The lowest apparent leaf temperature was found in *Tripleurospermum inodorum* (mean = 12.858 °C, SD = 0.528 °C) (Figure 1).

The correction index (T plant/T sand) also differed significantly among species ($F_{(9, 127)}$ = 124.35, P < 0.001), with a sum of squares of 0.420 for species and 0.134 for residuals. The residual standard error was 0.032 (Figure 2). The greatest temperature differences between plants and sand were found in the cereals – barley (mean = 1.148, SD = 0.029), sorghum (mean = 1.149, SD = 0.037) and wheat (mean = 1.144, SD = 0.042), followed by *Amaranthus retroflexus* (mean = 1.134, SD = 0.021) and *Echinochloa crus-galli* (mean = 1.128, SD = 0.022) (Figure 2).

Hyperspectral reflection. The species' spectral curves varied across several spectral regions, particularly in the blue and red portions of the spectrum (Figure 3). ANOVA across the 530–589 nm wavelength range reveals that the greatest interspecific differences occur at 550 nm (Table 1). However, differences in reflectance at this peak were not always significant among all species (Figure 4). No significant differences in 550 nm were observed between sorghum and *Echinochloa crus-galli*, or between barley, wheat, *Tripleurospermum inodorum* and *Veronica persica*. The highest reflectance at 550 nm was observed in oilseed rape (0.265 ± 0.044), followed by *Stellaria media* (0.228 ± 0.017) (Figure 4). The NDI also showed five distinct plant groups (Figure 5). The highest NDI

Table 1. ANOVA results for wavelengths 530–589 nm (model: aov(reflectance ~ species))

Wavelength (nm)	*df*	Sum of squares	Mean square	*F* value	*P*-value
530.96	9	0.6169	0.06855	55.01	< 0.001
533.89	9	0.6583	0.07315	57.54	< 0.001
536.82	9	0.6904	0.07671	58.94	< 0.001
539.75	9	0.7143	0.07937	60.72	< 0.001
542.68	9	0.7360	0.08178	62.28	< 0.001
545.62	9	0.7536	0.08373	63.15	< 0.001
548.55	9	0.7675	0.08528	63.44	< 0.001
551.49	**9**	**0.7604**	**0.08449**	**105.10**	**< 0.001**
554.43	9	0.7775	0.08639	64.35	< 0.001
557.36	9	0.7665	0.08516	63.92	< 0.001
560.30	9	0.7451	0.08279	63.48	< 0.001
563.24	9	0.7161	0.07957	61.51	< 0.001
566.18	9	0.6830	0.07588	59.83	< 0.001
569.12	9	0.6470	0.07189	57.52	< 0.001
572.07	9	0.6119	0.06799	55.65	< 0.001
575.01	9	0.5790	0.06434	53.57	< 0.001
577.96	9	0.5495	0.06105	51.76	< 0.001
580.90	9	0.5199	0.05777	50.09	< 0.001
583.85	9	0.4944	0.05493	48.03	< 0.001
586.80	9	0.4728	0.05253	46.84	< 0.001
589.75	9	0.4555	0.05061	45.37	< 0.001

The highest *F*-value was observed at 551.49 nm (≈550 nm), indicating maximal interspecific separation within the investigated window

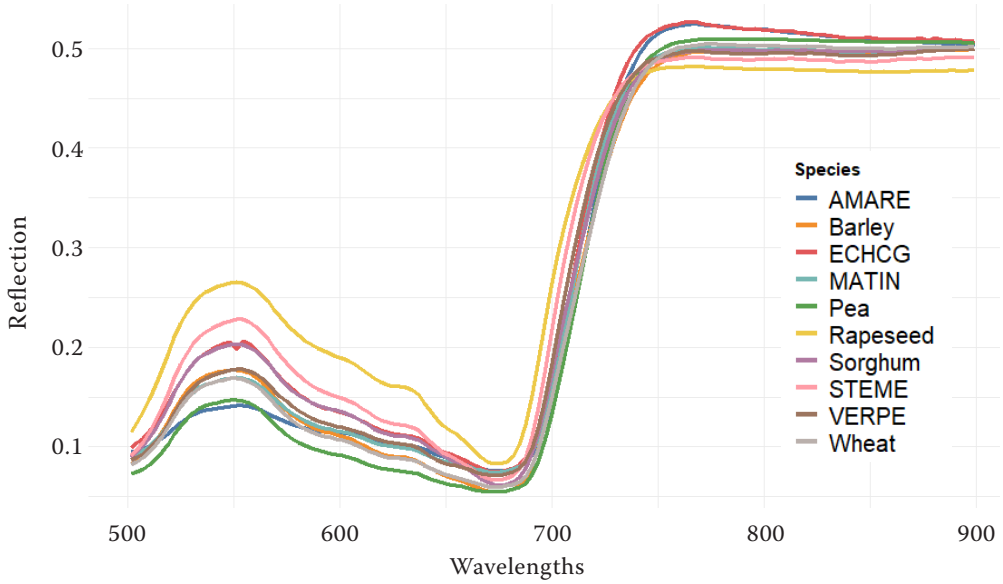

Figure 3. Mean hyperspectral reflection curves of weeds (AMARE – *Amaranthus retroflexus*; ECHCG – *Echinochloa crus-galli*; MATIN – *Tripleurospermum inodorum*; STEME – *Stellaria media*; VERPE – *Veronica persica*) and crops, showing the main peak at 550 nm

https://doi.org/10.17221/534/2025-PSE

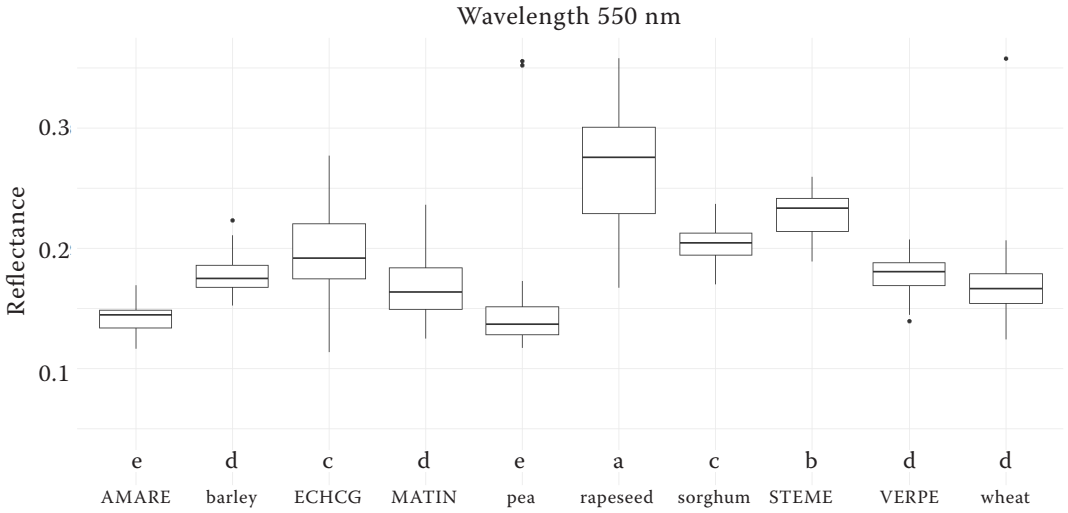

Figure 4. Reflectance of the plants at 550 nm. Letters above species names indicate statistically significant differences ($P < 0.05$). Boxes represent interquartile ranges, and horizontal lines indicate medians. AMARE – *Amaranthus retroflexus*; ECHCG – *Echinochloa crus-galli*; MATIN – *Tripleurospermum inodorum*; STEME – *Stellaria media*; VERPE – *Veronica persica*

values were similarly observed in oilseed rape, and the lowest in *Amaranthus retroflexus*.

DISCUSSION

In this study, apparent leaf temperature and hyperspectral reflectance were evaluated for differentiating weeds and crops. Both sensors showed different capacities to discriminate among species. In thermal imaging, the temperature patterns observed between species differed from those obtained through hyperspectral analysis.

Distinct apparent leaf temperatures were detected among plant species (Figures 1 and 2). The highest apparent leaf temperatures were found in the Poaceae family (barley, *Echinochloa crus-galli*, sorghum and wheat) and in *Amaranthus retroflexus*. Differences in leaf morphology between Poaceae and dicotyledonous species may influence transpirational cooling mechanisms (Krasser and Kalapos 2000).

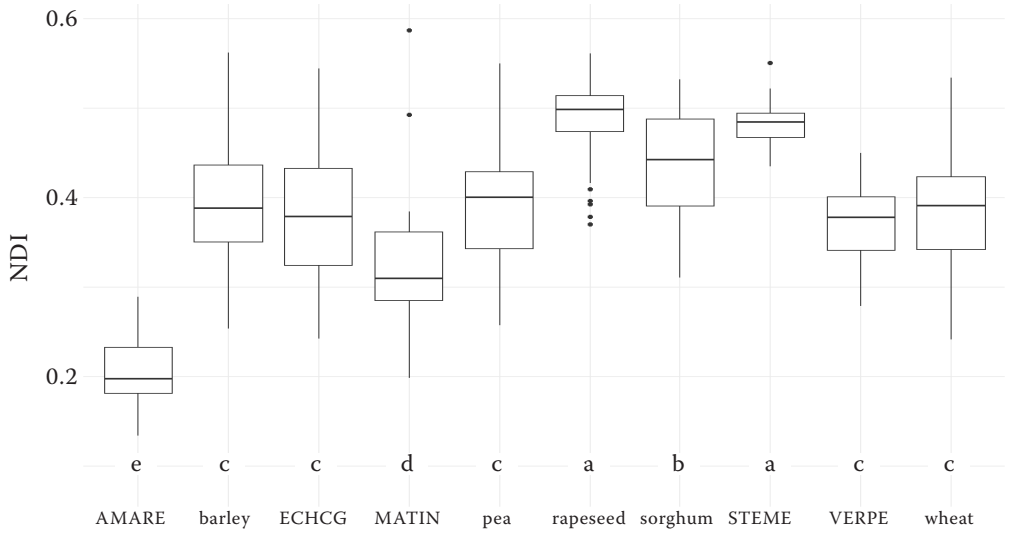

Figure 5. Normalised difference index (NDI). Letters above species names indicate statistically significant differences ($P < 0.05$). Boxes represent interquartile ranges, and horizontal lines indicate medians. AMARE – *Amaranthus retroflexus*; ECHCG – *Echinochloa crus-galli*; MATIN – *Tripleurospermum inodorum*; STEME – *Stellaria media*; VERPE – *Veronica persica*

https://doi.org/10.17221/534/2025-PSE

Weeds *Amaranthus retroflexus* and *Echinochloa crus-galli* differed from other dicotyledonous weeds, likely due to their different growth strategies. These two species germinate in late spring, whereas the remaining weeds (*Tripleurospermum inodorum*, *Veronica persica*, *Stellaria media*) are early-spring germinating species (Sobey 1981). Consequently, their leaf morphology and water regulation regime differ.

Both *Amaranthus retroflexus* and *Echinochloa crus-galli* are C4 plants (Sage and Pearcy 1987, Rao et al. 2007), whereas the other tested weeds are C3 (Carni and Mucina 1998). However, this pattern was not fully consistent in the crops: sorghum (C4 plant) did not differ in apparent leaf temperature after correction from the C3 cereal (wheat and barley) (Day and Parkinson 1982, Stefanov et al. 2022). The differences between C3 and C4 photosynthetic systems may affect thermal emission through variation in stomatal aperture (Shabala 1997) and uneven stomatal distribution within leaves. Additional factors, such as cuticular wax or oil content, may also influence thermal emission and heat regulation (Tassone et al. 2016).

Although some methodological issues were addressed through thermal correction, other sources of variation may have affected the results, such as heat reflection from surrounding objects, limitations of uncooled thermal sensors, or a low number of analysed pixels. Uncooled thermal cameras exhibit higher signal-to-noise ratios and lower image quality than cooled models; however, the latter are prohibitively expensive for agricultural use. In this study, the thermal camera had a thermal sensitivity of 0.03 °C (NETD = 30 mK), which may affect the repeatability/separability of the thermal signal and, therefore, weed detection.

Differences in hyperspectral reflectance were also detected among species (Figures 3–5). The pronounced variation occurred at 550 nm, in agreement with previous studies (Gitelson and Merzlyak 1998). The relative reflectance of wheat Saphira did not match the exact 550 nm values reported in this study. Still, the general spectral patterns were similar, with broadleaf weeds generally exhibiting higher reflectance values (Figures 3 and 4).

At 550 nm, some species were easily distinguishable from others (Figure 4). Oilseed rape exhibited the highest reflectance, consistent with the findings of Wei et al. (2014). This characteristic may be linked to the species' surface properties – superhydrophobicity, low adhesion, and self-cleaning ability (Zhu and Guo 2016) – and to the presence of a thick wax layer on its leaves (Tassone et al. 2016). No significant difference in 550 nm reflectance was found between sorghum and *Echinochloa crus-galli* (Figure 4). Their leaf morphology, particularly size, distribution or spatial arrangement, may produce similar spectral reflectance.

Tripleurospermum inodorum has a distinctive leaf structure: narrow, thread-like, and finely divided into several feathery, branching lobes (Grime et al. 1990). This morphology may influence both sensors' outputs, as analyses were conducted on the first true leaf, potentially introducing variations. The most notable challenge in hyperspectral detection was the lack of significant reflectance differences among wheat, barley, *Veronica persica*, and *Tripleurospermum inodorum.* The latter is one of the most problematic weeds in cereal crops (Hamouz et al. 2014). Similarly, in other hyperspectral studies, not all species could be discriminated; for instance, Dmitriev et al. (2022) reported no significant difference between *Atriplex vs. Glycyrrhiza* and *Euphorbia vs. Glycyrrhiza*.

Further studies should also focus on creating additional spectral indices that can better distinguish species from each other. As already mentioned, the technical aspects of spectral cameras and environmental conditions do not offer options that would allow the use of a single spectrum (Nansen et al. 2025). For this reason, it would be appropriate in future studies to create a sufficient sample that can be trained with neural networks, so that the best results are achieved.

Field-based hyperspectral weed detection may face additional challenges. In natural canopies, overlapping plant layers (crops above and weeds below) can lead to mixed pixels, increasing the risk of misclassifications, as observed in forest species studies (Modzelewska et al. 2020). Soil moisture variability and illumination intensities also influence spectral readings (El-Faki et al. 2000b). Moreover, herbicide application and pest infestation can alter plant physiology, modifying both hyperspectral and thermal responses. Herbicide exposure often induces stress, altering chlorophyll content and reflectance profiles (Scholten et al. 2019). However, changes in chlorophyll content may also arise from physiological differences or developmental stage (Gitelson and Merzlyak 1998).

In this study, all plants were grown in a controlled chamber with identical light cycles and spectra. Watering was adjusted by species, and no pest infestation occurred. These conditions ensured minimal stress, al-

https://doi.org/10.17221/534/2025-PSE

lowing valid interspecific comparisons. Future studies should explore changes in hyperspectral reflectance following herbicide treatment and differences between C3 and C4 plants under varied stress conditions.

Although modern sensor-based methods can already assist in weed recognition – for example, RGB-based diagnostics that rely on leaf shape, colour, or size (Pathak et al. 2023) – they have limitations. These include variation in leaf morphology due to mutation, herbicide protection, disease, or pest damage, as well as canopy overlap and environmental factors such as wind (El-Faki et al. 2000a). Since each approach has constraints, the most effective strategy for field weed detection will likely involve data fusion from multiple sensors. Given the high costs of hyperspectral systems, identifying a limited set of spectral bands with the greatest discriminatory power could facilitate the development of simpler, more affordable sensors.

While both thermal and hyperspectral sensors demonstrate strong potential for weed recognition, environmental factors such as wind, humidity, and rainfall can degrade data quality, and this should be considered in field applications.

Thermal and hyperspectral imaging can effectively differentiate among certain plant species. In thermal imaging, cereal crops exhibited higher apparent leaf temperature, while hyperspectral imaging showed the greatest interspecific variation at 550 nm, with oilseed rape displaying the highest reflectance. These patterns are attributed to differences in leaf morphology, taxonomy, and physiology. Although further validation is required under field conditions, the findings provide promising evidence for the development of advanced sensor-based weed detection systems.

Acknowledgement. We are thankful to Helena Uhlířová and Hana Smutná for great technical support.

REFERENCES

Barros-Rodriguez A., Rangseekaew P., Lasudee K., Pathom-aree W., Manzanera M. (2021): Impacts of agriculture on the environment and soil microbial biodiversity. Plants-Basel, 10: 2325.

Carni A., Mucina L. (1998): Vegetation of trampled soil dominated by C4 plants in Europe. Journal of Vegetation Science, 9: 45–56.

Catena A., Catena G. (2008): Overview of thermal imaging for tree assessment. Arboricultural Journal, 30: 259–270.

Chen F., Van de Voorde T., Roberts D., Zhao H., Chen J. (2021): Detection of ground materials using normalized difference indices with a threshold: risk and ways to improve. Remote Sensing, 13: 450.

Day W., Parkinson K.J. (1982): Application to wheat and barlex of 2leaf photosynthesismodels for C3 plants. Plant, Cell and Environment, 5: 501–507.

Dmitriev P.A., Kozlovsky B.L., Kupriushkin D.P., Dmitrieva A.A., Rajput V.D., Chokheli V.A., Tarik E.P., Kapralova O.A., Tokhtar V.K., Minkina T.M., Varduni T.V. (2022): Assessment of invasive and weed species by hyperspectral imagery in agrocenoses ecosystem. Remote Sensing, 14: 2442.

Eide A., Zhang Y., Koparan C., Stenger J., Ostlie M., Howatt K., Bajwa S., Sun X. (2021): Image based thermal sensing for glyphosate resistant weed identification in greenhouse conditions. Computers and Electronics in Agriculture, 188: 106348.

El-Faki M., Zhang N., Peterson D.E. (2000a): Weed detection using color machine vision. Transactions of the ASAE, 43: 1969–1978.

El-Faki M., Zhang N., Peterson D.E. (2000b): Factors affecting color-based weed detection. Transactions of the ASAE, 43: 1001–1009.

Espinoza C.Z., Khot L.R., Sankaran S., Jacoby P.W. (2017): High resolution multispectral and thermal remote sensing-based water stress assessment in subsurface irrigated grapevines. Remote Sensing, 9: 961.

Esposito M., Westbrook A.S., Maggio A., Cirillo V., DiTommaso A. (2023): Neutral weed communities: the intersection between crop productivity, biodiversity, and weed ecosystem services. Weed Science, 71: 301–311.

Gitelson A.A., Merzlyak M.N. (1998): Remote sensing of chlorophyll concentration in higher plant leaves. Synergistic Use of Multisensor Data for Land Processes, 22: 689–692.

Grime J.P., Hodgson J.G., Hunt R. (1990): The Abriged Comparative Plant Ecology. London, Chapman and Hall.

Hamouz P., Hamouzová K., Holec J., Tyšer L. (2014): Impact of site-specific weed management in winter crops on weed populations. Plant, Soil and Environment, 60: 518–524.

Habili N., Oorloff J. (2015): Scyllarus: from research to commercial software. ASWEC 2015, Adelaide, Australia, 119–122.

Khanal S., Fulton J., Shearer S. (2017): An overview of current and potential applications of thermal remote sensing in precision agriculture. Computers and Electronics in Agriculture, 139: 22–32.

Krasser D., Kalapos T. (2000): Leaf water relations for 23 angiosperm species from steppe grasslands and associated habitats in Hungary. Community Ecology, 1: 123–131.

Maimaitijiang M., Ghulam A., Sidike P., Hartling S., Maimaitiyiming M., Peterson K., Shavers E., Fishman J., Peterson J., Kadam S., Burken J., Fritschi F. (2017): Unmanned Aerial System (UAS)-based phenotyping of soybean using multi-sensor data fusion and extreme learning machine. ISPRS Journal of Photogrammetry and Remote Sensing, 134: 43–58.

Marschner C., Colucci I., Stup R., Westbrook A., Brunharo C., DiTommaso A., Mesgaran M. (2024): Modelling weed seedling emergence for time-specific weed management: a systematic review. Weed Science, 72: 313–329.

https://doi.org/10.17221/534/2025-PSE

Mesnage R., Zaller J.G. (2021): Herbicides: Chemistry, Efficacy, Toxicology, and Environmental Impacts. Amsterdam, Elsevier Science Publishing Co., Inc. ISBN: 978-0-12-823674-1

Modzelewska A., Fassnacht F.E., Sterenczak K. (2020): Tree species identification within an extensive forest area with diverse management regimes using airborne hyperspectral data. International Journal of Applied Earth Observation and Geoinformation, 84: 101960.

Murad N., Mahmood T., Forkan A., Morshed A., Jayaraman P., Siddiqui M. (2023): Weed detection using deep learning: a systematic literature review. Sensors, 23: 1.

Nansen C., Lee H., Mesgaran M.B. (2025): Experimental design issues associated with classifications of hyperspectral sensing data. Precision Agriculture, 26: 80.

Page E., Cerrudo D., Westra P., Loux M., Smith K., Foresman C., Wright H., Swanton C. (2012): Why early season weed control is important in maize. Weed Science, 60: 423–430.

Pantazi X.E., Moshou D., Bravo C. (2016): Active learning system for weed species recognition based on hyperspectral sensing. Biosystems Engineering, 146: 193–202.

Pathak H., Igathinathane C., Howatt K., Zhang Z. (2023): Machine learning and handcrafted image processing methods for classifying common weeds in corn field. Smart Agricultural Technology, 5: 100249.

Primel E.G., Zanella R., Kurz M.H.S., Goncalves F.F., Machado S.D., Marchezan E. (2005): Pollution of water by herbicides used in the irrigated rice cultivation in the central area of Rio Grande do Sul State, Brazil: theoretical prediction and monitoring. Quimica Nova, 28: 605–609.

Pu R., Gong P., Tian Y., Miao X., Carruther R., Anderson G. (2008): Using classification and NDVI differencing methods for monitoring sparse vegetation coverage: a case study of saltcedar in Nevada, USA. International Journal of Remote Sensing, 29: 3987–4011.

Raja R., Nguyen T.T., Slaughter D.C., Fennimore S.A. (2020): Real-time weed-crop classification and localisation technique for robotic weed control in lettuce. Biosystems Engineering, 192: 257–274.

Rao A.N., Johnson D.E., Sivaprasad B., Ladha J.K., Mortimer A.M. (2007): Weed management in direct-seeded rice. Advances in Agronomy, 93:153.

Sage R.F., Pearcy R.W. (1987): The nitrogen use efficiency of C3 and C4 plants: II. Leaf nitrogen effects on the gas exchange characteristics of *Chenopodium album* (L.) and *Amaranthus retroflexus* (L.). Plant Physiology, 84: 959–963.

Scholten R.C., Hill J., Werner W., Buddenbaum H., Dash J.P., Gallego M.G., Rolando C.A., Pearse G.D., Hartley R., Estarija H.J., Watt M.S. (2019): Hyperspectral VNIR-spectroscopy and imagery as a tool for monitoring herbicide damage in wilding conifers. Biological Invasions, 21: 3395–3413.

Shabala S.N. (1997): Leaf bioelectric responses to rhythmical light: identification of the contributions from stomatal and mesophyll cells. Australian Journal of Plant Physiology, 24: 741–749.

Shirzadifar A. (2018): Identification of weed species and glyphosate-resistant weeds using high resolution UAS Images. [Ph.D. thesis] North Dakota, NDSU. Available at: https://library.ndsu.edu/ir/handle/10365/29304

Shoba S., Pandiyarajan T., Shashidhar K. (2024): Nondestructive detection of fruit fly (*Bactrocera dorsalis*) infestation in Alphonso and Totapuri varieties of mango fruits by thermal imaging technique. Journal of Food Process Engineering, 47: 14610.

Sobey D.G. (1981): *Stellaria media* (L.) Vill. Journal of Ecology, 69: 311–335.

Stajnko D., Lakota M., Hocevar M. (2006): Application of thermal imaging for visualization of high density orchards and counting apple fruits. Acta Horticulturae, 707: 211–215.

Stefanov M.A., Rashkov G.D., Apostolova E.L. (2022): Assessment of the photosynthetic apparatus functions by chlorophyll fluorescence and P700 absorbance in C3 and C4 plants under physiological conditions and under salt stress. International Journal of Molecular Sciences, 23: 3768–3768.

Su W. (2020): Advanced machine learning in point spectroscopy, RGB- and hyperspectral-imaging for automatic discriminations of crops and weeds: a review. Smart Cities, 3: 767–792.

Tassone E.E., Lipka A.E., Tomasi P., Lohrey G.T., Qian W., Dyer J.M., Gore M.A., Jenks M.A. (2016): Chemical variation for leaf cuticular waxes and their levels revealed in a diverse panel of *Brassica napus* L. Industrial Crops and Products, 79: 77–83.

Taylor J., Mills M., Burns R. (2004): Sorption and desorption behaviour of acetochlor in surface, subsurface and size-fractionated soil. European Journal of Soil Science, 55: 671–679.

Team R.C. (2022): R: A Language and Environment for Statistical Computing. Vienna, Austria: R Foundation for Statistical Computing.

Thenkabail P., Gumma M., Teluguntla P., Ahmed M.I. (2014): Hyperspectral remote sensing of vegetation and agricultural crops. Photogrammetric Engineering and Remote Sensing, 80: 695–723.

Wang A.C., Zhang W., Wei X.H. (2019): A review on weed detection using ground-based machine vision and image processing techniques. Computers and Electronics in Agriculture, 158: 226–240.

Wei D., Mei J., Fu Y., Disi J., Li J., Qian W. (2014): Quantitative trait loci analyses for resistance to *Sclerotinia sclerotiorum* and flowering time in *Brassica napus*. Molecular Breeding, 34: 1797–1804.

Zhu H., Guo Z.G. (2016): Wetting characterizations of oilseed rapes. Journal of Bionic Engineering, 13: 213–219.

Received: November 27, 2025
Accepted: February 9, 2026
Published online: February 24, 2026